Available online at www.sciencedirect.com
ScienceDirect
Trans. Nonferrous Met. Soc. China 22(2012) s838−s844
Transactions of Nonferrous Metals Society of China
www.tnmsc.cn

Deformation prediction of porcelain-enameled steels with strain history by press forming and high-temperature behavior of coating layer

Young-Ki SON[1], Chan-Joo LEE[2], Jung-Min LEE[2], Byung-Min KIM[1]

1. School of Mechanical Engineering, Pusan National University, Busan 609-735, Korea;
2. Dongnam Regional Division, Korea Institute of Industrial Technology, Busan 618-230, Korea

Received 21 May 2012; accepted 6 November 2012

Abstract: Porcelain enamel coatings were widely applied for the protection of steel products because they offered high corrosion protection, resistance to heat and abrasion, high hardness, hygiene and ease of cleaning. The typical process to produce enameled steels is roughly divided into two stages: the first stage consists of a forming process to give the desired shape to a steel substrate, and the second stage consists of a firing process to bond enamel frits on the substrate. This firing process requires a high temperature above 800 °C, which may lead to austenitic transformation and severe thermal deformation of the steel substrate. The aim of this study is to develop a finite element analysis (FE analysis) technique to predict the mechanical and thermal deformations of the enameled steels during forming and any further enameling process, including firing. The FE analysis involves analyzing the strain history of the steel substrate, which comprises the stress and thickness distributions of the substrate and its deformed shape, and the high-temperature behavior of the enamel coating layer. The validity of the FE analysis is verified through the U-bending test and firing test with various numbers and positions of enamel coating layers on the substrate. The results reveal that the FE analysis results agree well with the experimental results with 8% error.
Key words: porcelain enamel; firing process; finite element analysis; enameled steel; thermal deformation

1 Introduction

In industries, porcelain enamel coatings were widely applied for the protection of steel products from surrounding environments. This coating not only provides an aesthetic exterior but also provides excellent engineering properties, such as corrosion protection, resistance to heat and abrasion, hygiene and ease of cleaning. Enamel is essentially a glass with a low softening temperature of 510−530 °C. Thus, it is primarily used in kitchen utensils and heating systems that have a relatively low working temperature [1−4].

For cold or hot-rolled steel, typical commercial enameling consists of a two-stage process (2 coat/1 fire or 2 coat/2 fire enameling), in which a ground coating is followed by a further coating (cover coating) of glass frit. Each coating is wet or dry sprayed on the steel surface in order, dried, and then fired at approximately 800 °C for 3−4 min. This firing temperature is very close to the austenitic transformation range of steels. Thus, enameling steels should contain a low carbon concentration (not over 0.12%), which results in low strength and high elongation of the metal. The carbon content of enameling steels can decrease up to 0.018% when Ti, Nb, Zr or B is added to it [5−9].

The characteristics of enameled steels after enameling are very similar to those of bi-metals. This can occasionally lead to unexpected distortions and excessive residual stress of the final enameled products. These problems may worsen as the enameling on steels gets thinner and the shape of enamel-related parts becomes more complicated. Typical defects of enameled parts are chipping, crazing warping, and spalling of the enamel coating. In many instances, most of these problems occur after firing or final assembly and are caused by the residual stress distributions of the enameled parts [10,11].

The distortion and the residual stress of the enamel-steel system mainly depend on the high-temperature behavior of the enamel and steel substrate, the complexity of the enameled parts, the strain history

Foundation item: Project (NRF-2012R1A5A1048294) supported by the National Research Foundation of Korea(NRF) Grant funded by the Ministry of Education, Science and Technology, and the LG Electronics
Corresponding author: Byung-Min KIM; Tel: +82-51-5103074; E-mail: bmkim@pusan.ac.kr
DOI: 10.1016/S1003-6326(12)61813-5

of the steel substrate, and the application environments, as shown in Fig. 1. The enamel-steel system has compressive stresses at its interface at room temperature. The enamel frits have lower thermal expansion than the steel. However, the enamel expansion becomes greater than that in steel as the enamel reaches its glass transition point. The enamel is under tension during the initial cooling state immediately after firing [12]. When it is gradually cooled to room temperature, the tension in the enamel changes into compression below the glass transition temperature (T_g) (Fig. 2). Thus, the proper control of the distortions and the residual stress of the enamel-steel system is one of the most important factors in determining the longevity of the enameled part.

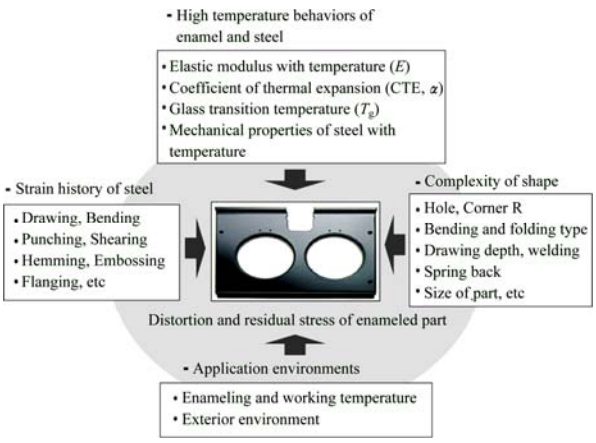

Fig. 1 Factors affecting distortion and residual stress of enameled products

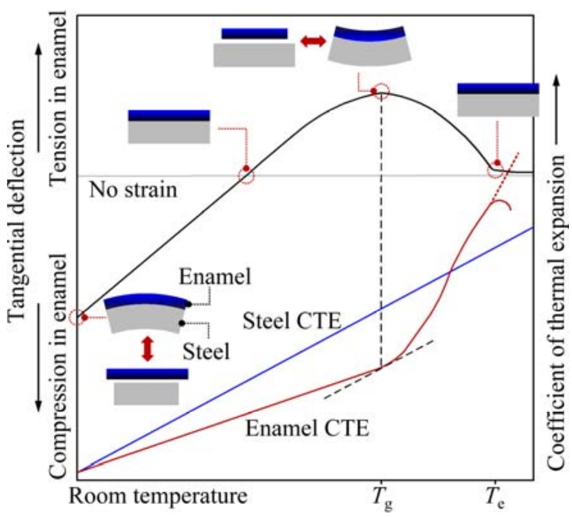

Fig. 2 Distortions and residual stress, thermal expansion of enamel-steel system with temperatures

This study was designed to develop an FE analysis technique for predicting the mechanical and thermal deformations of enameled steels, including their strain history, by press forming and the behavior of the coating layer. A U-bending model was chosen as the FE model to simplify the deformation measurement of the enameled part in the FE simulations. In addition, the deformation of the enameled part was estimated for various positions and number of coating layers on the steel substrate. Finally, to verify the reliability of the FE analysis, a U-bending test of the steel substrate and the enameling process are performed.

2 FE analysis and experiments

2.1 Procedure of FE analysis

Figure 3 shows the FE analysis procedure for predicting the deformation of the enameled steel through the entire fabrication processes. The FE simulations were composed of a press forming, spring-back, and enameling process analyses. First, press forming used to bend a steel strip into a U-shape analyzed; this analysis was followed by the calculation of spring-back in the U-shaped strip after removing the punch and die. This U-shaped strip with its strain histories (strain and thickness distributions) and elastic recovery was used as the initial FE model for further enameling analysis. Moreover, the mechanical properties of this strip such as flow stress, elastic modulus (E), Poisson ratio (v), and the coefficient of friction (μ) were used as the input values for the press forming analysis.

In the enameling process, enamel frits dry-sprayed on steel will not substantially affect the thermal deformation of the steel substrate during heating from room temperature to 800 °C because the frits behave as viscous fluids at that temperature. Thus, after spring-back analysis, the U-shaped model without any enamel coating was heated to the temperature of 800 °C (first heating, a to b' section). The enamel-coating layer (ground coat, b' to b'' section) was then created on the thermally deformed model, and the model with this new coating layer was again cooled to room temperature (first cooling, b'' to c' section). In the same way, after the fist cooled model was reheated to 800 °C (second heating, c' to d' section), a cover coating layer was formed on the model (d' to d'' section). Lastly, the model with both the ground and the cover coating layers was re-cooled to room temperature (second cooling, d'' to e section). The mechanical properties at elevated temperatures such as flow stress, elastic modulus (E), Poisson ratio (v), and coefficient of thermal expansion (CTE) were used as the inputs in the enameling process analysis. In Fig. 3, the outputs calculated from each analysis, which are the strain and thickness distributions and the deformed shapes, are continuously recorded during a series of FE simulations. Therefore, the final second cooled model can be expected to represent the final mechanical and thermal deformations of the enameled part, because it

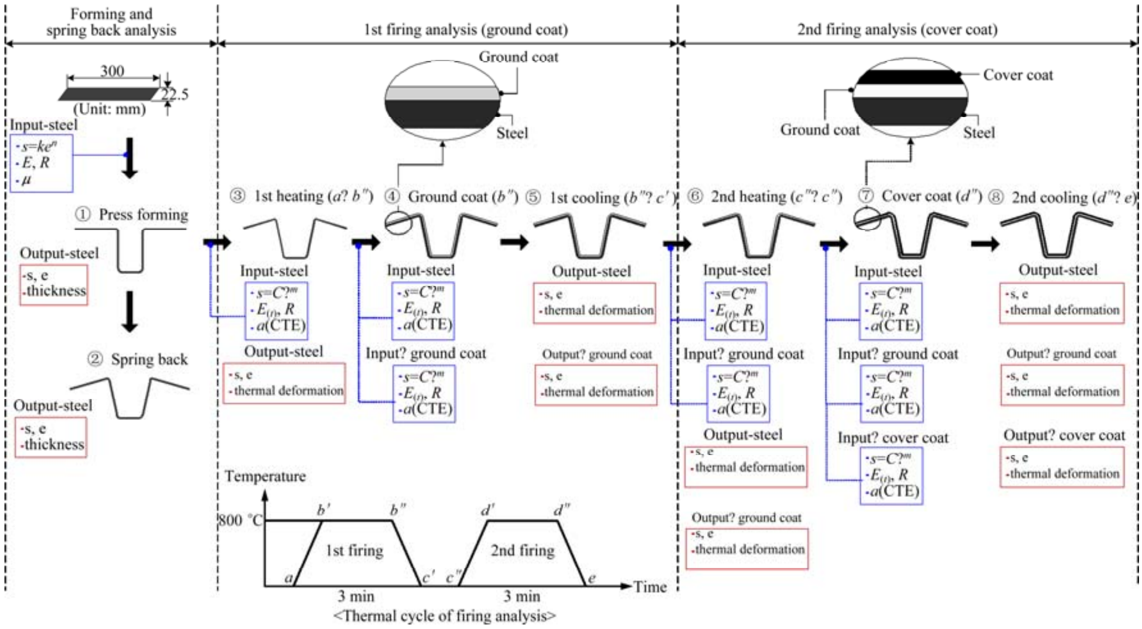

Fig. 3 Procedure of FE analysis to predict deformation of enameled steel during forming and enameling processes

has all the strain histories for the press forming, spring-back, and the first and second firing processes.

2.2 Conditions and models of FE analysis

Figure 4 shows the dimensions and FE models of the punch, die, and holder for the press forming and spring-back analysis of the steel. An initial steel strip (300 mm (L) × 22.5 mm (W) × 0.7 mm (T)) was formed into U-shape by press forming and its spring-back was estimated immediately after releasing from the die. All the FE models were generated using 4-node shell elements and were assumed to be only half sections, taking into consideration bilateral symmetry.

Figure 5 exhibits the first and second heated steel substrate with coating layers after performing the spring-

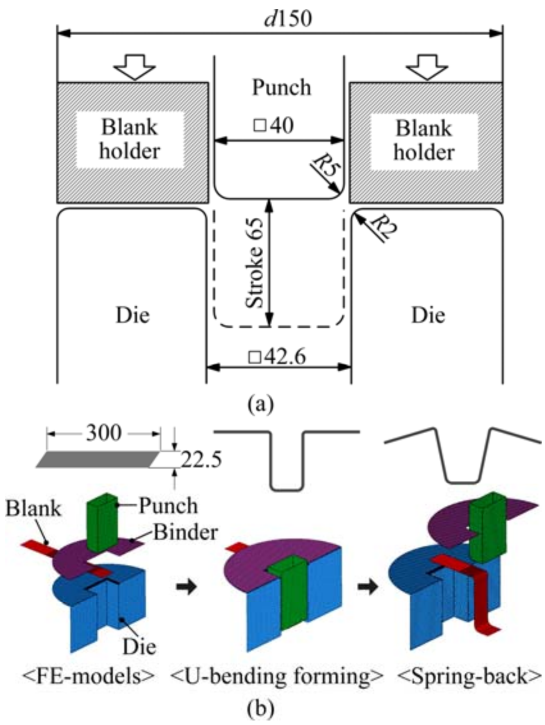

Fig. 4 FE models of press forming and spring- back analysis: (a) Dimensions of U-bending model; (b) FE models (Unit: mm)

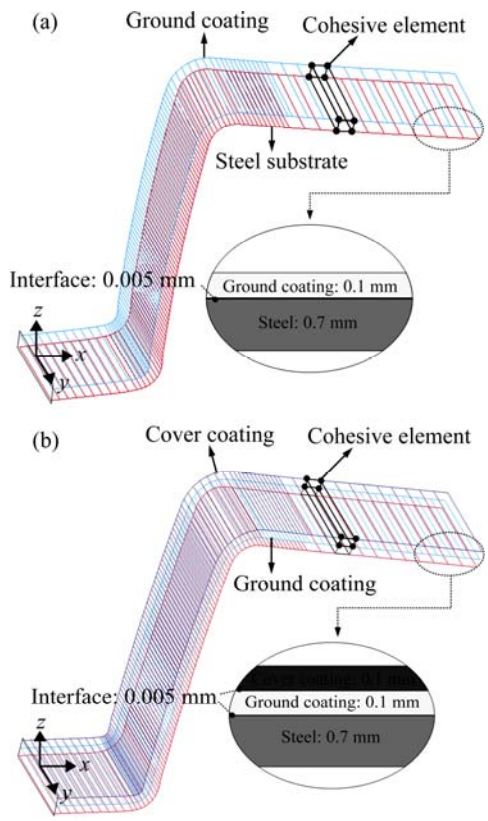

Fig. 5 FE models of enameled steel with coating layer: (a) 1st heating; (b) 2nd heating

back analysis shown in Fig. 3. These coatings were also generated using 4-node shell elements and located on the substrate by 0.1 mm offset. For a link between the ground and the cover coatings (or the substrate and ground coating), the interfacial layers were created using 8-node solid elements with thickness of 0.005 mm. The thicknesses of the coatings and the substrate were 0.1 and 0.7mm, respectively.

In this study, the conditions of enamel coatings fused on the steel substrate are summarized in Fig. 6. A total of seven enameled steel specimens were produced for various positions and the number of enamel coatings on the substrate. However, the firing processes performed in this study are 1 coat/1 fire and 2 coat/2 fire processes for the number of coatings, and the regardless of their positions. The final deformations of these enameled steels were quantitatively estimated through the FE simulations shown in Fig. 3.

Simulation conditions of the press forming and the firing processes are summarized in Table 1. The blank holding force (BHF) was 5 kN and the frictional coefficient between the steel and die was 0.125. The steel strip was formed at a punch speed of 5 mm/min until the punch stroke was 65 mm. During the spring-back analysis, the symmetrical planes of the deformed steel were perfectly constrained by *x*, *y* and *z* displacements of 0. In the firing process analysis, the steel and the coatings

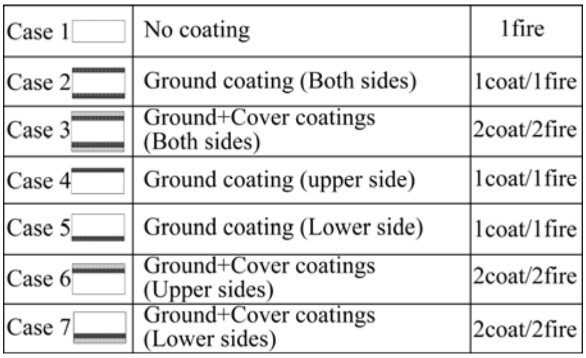

Fig. 6 Conditions of enamel coating on steel substrate

Table 1 Conditions of FE analysis

Press forming analysis	
Material	CESP-C ($\sigma = 512.11 \cdot \varepsilon^{0.269}$ MPa)
Poisson ratio (v)	0.3
Coefficient of friction (μ)	0.125
Punch speed	5 mm/min
BHF	5 kN
Boundary conditions	Symmetrical plane: *xyz*=0 (Spring back analysis)
Firing process analysis	
Firing cycle	25 °C→800 °C(3 min)→25 °C
Boundary conditions	Symmetrical plane: *xyz* =0

were linearly heated from a room temperature (25 °C) to 800 °C for 25 s and cooled at a uniform rate for 25 s. The boundary conditions were equal to those for the spring-back analysis and the identical temperature conditions were imposed on all nodes of the FE models. Additionally, the softening of the steel and the coatings over time is not considered in this study. The press forming and spring-back analysis were performed using LS-DYNA and the firing process analysis was carried out using ABAQUS dynamic-explicit.

2.3 Material properties

The enameling steel used in this study was a low carbon steel with 0.0018% C, which is a commercial steel sheet (CESP-C) manufactured at POSCO (Korea). Its chemical compositions are listed in Table 2. Figure 7 shows the high-temperature flow stress curves of the enamel steel which were obtained from the tensile test. Its tensile strength and elongation were 320 MPa and 34%, respectively, at room temperature.

The chemical compositions of the ground and cover coatings are summarized in Table 3. The enamels used in this study have a commercial composition based on SiO_2, B_2O_3, KsO, and other oxides, and are widely used for kitchen utensils.

Table 2 Chemical compositions of enameling steel substrate

Alloy	Mass fraction/%						
	C	Mn	P	S	N	Cu	Ti
Low carbon steel	0.0018	0.130	0.011	0.031	0.0082	0.033	0.110

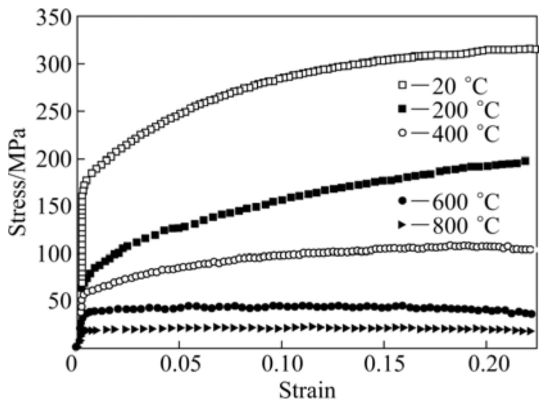

Fig. 7 True stress—true strain curves of enameling steel at elevated temperatures

Table 3 Chemical compositions of enamel frits

Coat	Mass fraction/%								Other components
	SiO_2	B_2O_3	K_2O	Na_2O	Al_2O_3	TiO_2	CoO	CaO	
Ground coat	48	12	3.2	13	2.3	3.6	1.5	2.8	5.6Li_2O; 2.5NiO
Cover coat	45	15	5.8	7.4	3.5	3.2	1.5	3.2	0.27Li_2O

Figure 8 shows the coefficients of thermal expansion (CTE) and the elastic modulus (E) of the steel and enamel at the elevated temperatures. The values for the enamel shown in Fig. 8 are substantially higher than those of the cover coating drawn from existing references. Although the ground and cover coatings have slightly different chemical compositions, they have the almost same elastic modulus at room temperature. Therefore, in this study, the ground and cover coatings are assumed to have the same mechanical and thermal characteristics for convenient FE simulations.

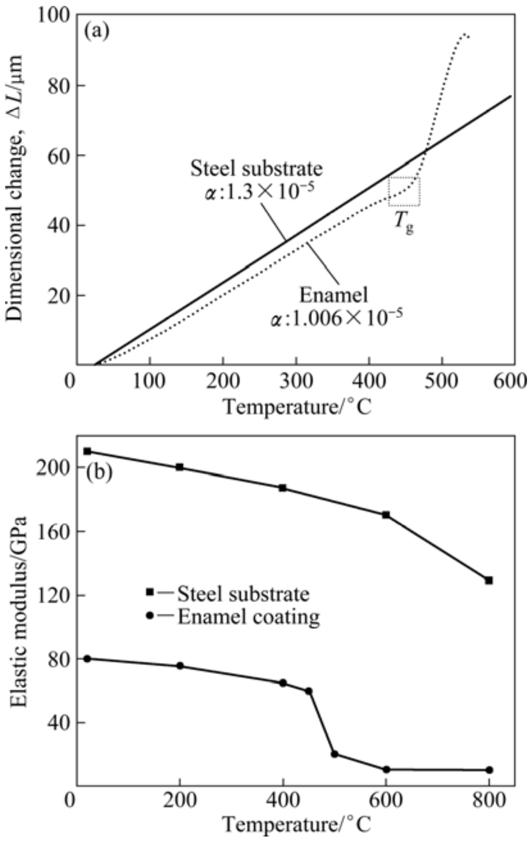

Fig. 8 True stress—true strain curves of enameling steel at elevated temperatures: (a) Thermal expansion; (b) Elastic modulus

The enamel does not have any stress in itself after the glass transition temperature of 450 °C because its behavior is similar to that of a viscous fluid. To reproduce this property, its elastic modulus above 450 °C is defined as approaching zero.

The normal stress, shear stress and elastic modulus of the interface, which are the critical values of cohesive element for debonding the interface, are 10 MPa, 5 MPa and 3 GPa, respectively. These values are arbitrarily set without taking into consideration delamination and fracture of the enamel coating including interface.

2.4 U-bending test and enameling process

The U-bending test of the steel was performed using a universal sheet forming tester (USM 500D). The shape of the tools and the general conditions of the test were identical to those of the press forming analysis.

Figure 9 shows that the U-shaped specimen elastically recovered after testing. Figure 10 shows the procedure of the enameling process for the U-shaped specimen after testing. The enameling process consisted of spraying, dehydration, firing, and cooling orders. The enamel slips used in this study were identical those listed in Table 2 and were produced by a ball mill process. The enamel slips were dry-sprayed on the steel substrate by electrostatic spraying at a high voltage (70 kV), with an average thickness of 0.1 mm. After being dehydrated, the steel substrate covered by the enamel slip passed through the open-type heating furnace, which has a firing zone of 800 °C, for about 3 min to obtain the enameled steel.

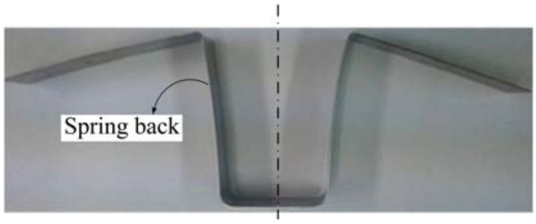

Fig. 9 U-shape specimen after spring-back

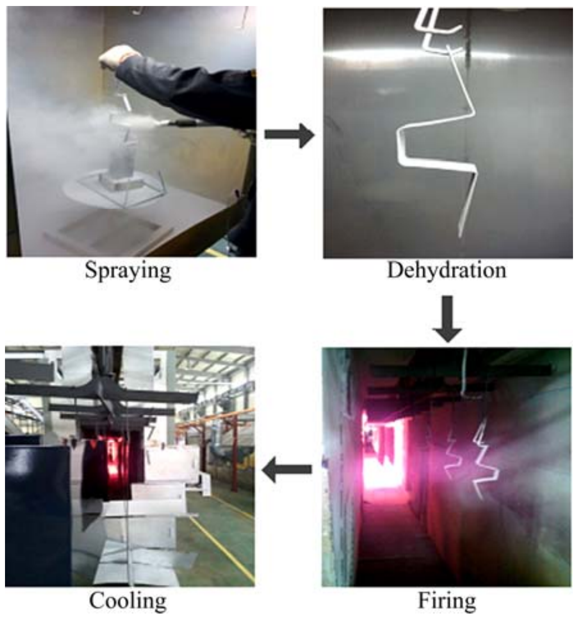

Fig. 10 Enameling process

3 Results and discussion

The spring-back of the specimen after the U-bending test is typically evaluated as θ_1 as shown in Fig. 11. Thus, to compare quantitatively the results of the FE analysis and the experiments, the deformation of the enameled steel is also defined as θ_1. Figure 12 shows the θ_1 values for all the enameled steels shown in Fig. 6 after enameling. The results show that the FE analysis provided slightly smaller values for θ_1 (0.4°−0.8°) than the experiments. However, enameled steels showed the same deformation behavior in both the FE simulations and the experiments for various conditions of enameling process.

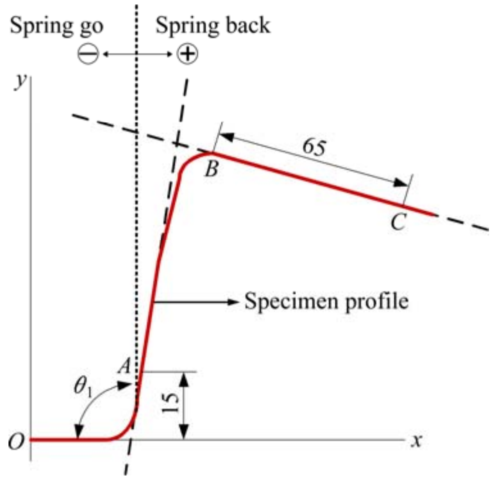

Fig. 11 Deformation measurements of enameled steels (Unit: mm)

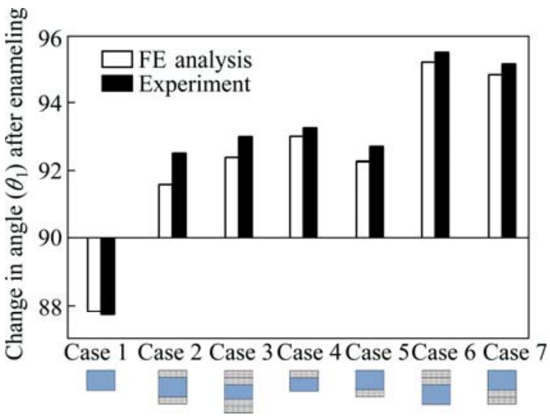

Fig. 12 Variations of θ_1 values for enameled steels

The differences between the experiment and the FE analysis are estimated to be mainly caused by the inaccurate material properties used in this study. The properties of the interface and the ground coatings in Fig. 8 are not accurate values obtained from the experiments but are only approximate. However, for the steel without coating (Case 1), the FE analysis results agreed very well with the experimental results, with less than 4% error, because its mechanical properties were directly determined from tensile tests.

Therefore, it is believed that the accuracy of the FE analysis would be improved if the actual properties of the interface and the coatings are applied.

The deformations of enameled steels primarily depend on the differences between the thermal expansions of the steel and enamel. As mentioned above, lower thermal expansion of the enamel restrains the contraction of the steel during cooling and results in moments that make the enameled steels curved at room temperature (Fig. 13). At this point the enamel and steel are under compressive and tensile stress, respectively.

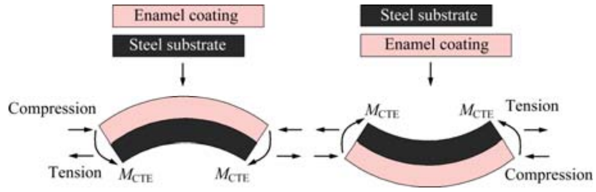

Fig. 13 Deformation behaviors of enameled steel by enamel coating

For the steel without the coating layer (Case 1), the steel is deformed by its thermal expansion in the $+\theta_1$ direction during heating but the steel recovers by its contraction in the $-\theta_1$ direction after cooling. On the other hand, enameled steels with a coating layer (Cases 2−7), have the same deformation in the $+\theta_1$ direction as that of the steel alone during heating. However, their final deformations appear to be in the $+\theta_1$ direction by resistance of the enamel coating to the thermal contraction of the steel during cooling.

For the upper (Cases 4 and, 6) and lower (Cases 5 and 7) coatings, their deformations (θ_1) rely on the locations of the coating. The upper coating leads to positive moments ($+M_{CTE}$) in the enameled steel, whereas the lower coating results in negative moments ($-M_{CTE}$). During cooling, the coatings obstruct the contraction of the steel on its upper and lower surfaces, respectively. Thus, the upper coating exhibits a larger deformation than the lower coating because its moment acts in the opposite direction to that in which the steel is contracted. For Cases 4 and 5, in which only one side is coated, and Case 2, in which both sides are coated, Case 2 has a smaller deformation than Cases 4 and 5 because the positive and negative moments are countervailed during cooling. In terms of the number of coatings, 2 coat/2 firing (Cases 3, 6, and 7) has a larger θ_1 value than 1 coat/1 firing (Cases 2, 4, and 5). This is because the samples undergoing the 2 coat/ 2 firing process are more thermally deformed by the two firing processes and therefore have more resistance to the thermal contraction of the steel by two coatings during cooling. Consequently, Case 7, which has two upper coating layers on one side of the steel, has the greatest deformation among all enameled steels.

Overall, the FEA technique established in this study reproduce the real mechanical and thermal behavior of enameled steels well for various conditions of the enameling process. Therefore, the technique is estimated to be a useful and effective method for predicting and controlling the deformation of enameled products such as cook-top plates, ranges, and oven trays, which are very complicated kitchen utensils.

4 Conclusions

1) In enameled steel at room temperature, because of lower thermal expansion of the enamel restrains, the contraction of the steel with relatively higher expansion during cooling, the steel and enamel are under compressive and tensile stresses, respectively. These stress conditions finally result in the curved deformation of the enameled steel, the direction of which depends on where the enamel coating is placed (upper or lower surfaces of the steel)

2) The deformation of enameled steel is smaller when both sides are coated and fired once than when one side is coated and fired twice, because each coating offsets the compressive stresses on the steel from the other coating, and single firing has a shorter heating time.

3) As compared with experiments, FE simulations provide relatively accurate deformation behavior and amount for the enameled steels, with less than 8% error. Thus, the FEA technique established in this study is estimated to be an effective method for predicting and controlling the deformation of enameled products.

References

[1] ANDREA Z, GIANGIACOMO M, DANIELE G. Low-velocity impact behavior of vitreous-enameled steel plate [J]. International Journal of Impact Engineering, 2010, 37: 673−684.

[2] WILLIAM D F. Stress and strain in enamel-steel composites: A practical viewpoint [J]. Porcelain Enamel Institute Technical Forum, 1997, 59: 101−111.

[3] JOHN J J, ANTHONY R M. Stress reduction in porcelain steel system [J]. Porcelain Enamel Institute Technical Forum, 1998, 60: 63−68.

[4] TSUI Y C, CLYNE T W. An analytical model for predicting residual stresses in progressively deposited coatings (Part 1): Planar geometry [J]. Thin Solid Films, 1997, 306: 23−33.

[5] LIU H H, SHEN P. Interdiffusion-induced devitrification of porcelain enamel on steel [J]. Journal of Materials Science, 1993, 28: 2105−2111.

[6] YANG X, JHA A, ALI S, COCHRANE R C. Mass-transport processes at the steel-enamel interface [J]. Metallurgical and Materials Transactions B, 2006, 37: 89−98.

[7] ISHIGURO Y, SUGIHARA R, TAHARA K, KUROKAWA T, HOSOYA Y. Adhesion of enamel layer after repeated firing in Ti-stabilized IF steel sheet for porcelain enamel use and its mechanism [J]. ISIJ International, 2004, 44: 1767−1773.

[8] SHARDAKOV N T, KURUMCHIN E K H, VDOVIN G K, DERYABIN V A. Effect of the steel substrate on the composition of gases in enameling [J]. Glass and Ceramic, 1996, 53: 46−47.

[9] FROLENKOV K Y, FROLENKOVA L Y, SHADRIN I F. High-temperature oxidation of low-alloyed steel under glass coatings [J]. Protection of Metals and Physical Chemistry of Surfaces, 2010, 46: 103−109.

[10] WANG D. Effect of crystallization on the property of hard enamel coating on steel substrate [J]. Applied Surface Science, 2009, 255: 4640−4645.

[11] SHIRASAKI M, SHIMIZU T. Evaluation method for the adhesion strength of vitreous enamel [J]. Journal of Materials Science, 1999, 34: 209−212.

[12] SAMIEE L, SARPOOLAKY H, MIRHABIBI A. Microstructure and adherence of cobalt containing and cobalt free enamels to low carbon steel [J]. Materials Science and Engineering A, 2007, 458: 88−95.

(Edited by HE Xue-feng)